Pergamon

Int. J. Solids Structures Vol. 35, Nos 31–32, pp. 4067–4075, 1998

0020–7683/98 $19.00 + .00

PII: S0020–7683(97)00301–6

MODELING THE CYCLIC LOADING RESPONSE OF SEA ICE

DAVID M. COLE*

Applied Research Division, U.S. Army Cold Regions Research and Engineering Laboratory, Hanover, NH, Germany

(*Received* 6 *November*, 1996; *accepted* 16 *June* 1997)

Abstract—This paper describes a physically based model of the elastic and anelastic behavior of sea ice subjected to zero-mean-stress cyclic loading. It incorporates the influence of porosity and fabric. The work demonstrates that despite the complexity of the sea ice microstructure, it is possible to develop links between its physical and mechanical properties through careful experimentation and detailed physical properties measurements.

As a consequence of the presence of liquid brine at temperatures of interest, the porosity of this material is temperature-dependent. The model accounts directly for the influence of temperature on the effective elastic properties (both through the lattice constants and through the total porosity), and on the dominant dislocations and grain boundary relaxation processes. It is shown via compliance measurements that the strength of the dislocation relaxation (and by inference the grown-in dislocation density) increases dramatically with the brine porosity.

Naturally occurring sea ice grown in the presence of a current offers the further complexity that the *c*-axes of the constituent hexagonal crystals tend to align themselves with the direction of the current. Because of the overwhelming ease of slip on the basal plane relative to other slip systems, the fabric thus produced has major influence on the mechanical properties. This effect of fabric has been incorporated in the model and verified with laboratory experiments on aligned sea ice specimens.

Discussion centers on the physical basis of the model and it is shown that the model predictions compare favorably with the available experimental data. © 1998 Published by Elsevier Science Ltd. All rights reserved.

1. INTRODUCTION

This paper presents recent advancements in the physically based modeling of the constitutive behavior of first-year sea ice. Attention focuses on elastic and anelastic straining under uniaxial, zero-mean-stress cyclic loading conditions. The cyclic loading method is particularly useful in this application since it produces sufficiently high strains to engage the dominant relaxation mechanisms without altering the physical characteristics of the specimen.

Sea ice has a complex flaw structure that changes with time and temperature. As a consequence of the growth process, it exhibits strong gradients in grain size and fabric. In addition, naturally occurring variations in growth rate cause corresponding variations in the liquid brine and gas content through the thickness of an ice sheet. All these factors influence the constitutive behavior of the ice and have been incorporated explicitly in the physically based model described below.

The model is based on laboratory studies of mechanical properties over a wide range of salinity. Extending the experimental work to very low and high brine contents—beyond the salinity extremes typically found in first-year sea ice—produces a more complete picture of the influence of this critical physical quantity on the mechanical behavior of sea ice. A careful examination of the mechanical behavior at very low brine porosities makes it possible to formulate a model that yields freshwater ice behavior as the brine porosity vanishes.

An ultimate goal of this effort is to develop, and verify at large scales, a model of the constitutive behavior of first-year sea ice that is based on readily determined physical properties. This work is part of a broader effort directed toward the development and

*E-mail: dmcole@crrel41.crrel.usace.army.mil.

verification at large scales of fracture and constitutive models for sea ice. An overview of the associated field program appears in Cole *et al.* (1995). Dempsey (1996) and Adamson and Dempsey (1996) present observations and analysis from that program regarding scale effects on the constitutive and fracture behavior of aligned first-year sea ice.

2. BACKGROUND

A series of studies (Cole and Durell, 1995; Cole, 1993, 1995, 1996; Cole *et al.*, 1996) was conducted to examine the relationship between the physical and mechanical properties of sea ice in detail. This section briefly highlights the key findings of those studies. The reader is referred to Cole (1996) for a more comprehensive background treatment of this topic.

Sea ice grows dendritically and as it solidifies, it incorporates liquid brine and gas inclusions predominantly along platelet boundaries. Specimens are typically characterized by the meltwater salinity and bulk density. These quantities allow the calculation of the brine and gas porosities (v_b and v_a, respectively) from published relationships (Cox and Weeks, 1983). Table 1 lists several important physical properties of sea ice and illustrates the various links to the mechanical properties and model quantities that are considered in the following sections.

It has long been recognized that sea ice is considerably more compliant than freshwater ice and the analysis of Cole (1995) associated the higher compliance with an increased dislocation density. It is uncertain whether the higher dislocation density is a consequence of the complex solidification process or their production at brine inclusions (Picu *et al.*, 1994). However, it is evident from the cyclic loading experiments of Cole and Durell (1995) that a power law relationship exists between brine porosity and compliance (Fig. 1). The power law exponent was found to be ≈ 2 in an analysis presented in Cole (1996). The curves in Fig. 1 are discussed in a subsequent section.

Individual crystals in an ice sheet exhibit a preferred orientation (fabric) when sea ice grows under the influence of a current. This produces aligned sea ice and it exists on a large scale in polar regions (Peyton, 1996; Weeks and Gow, 1979). Fabric development is found in glacier ice as a result of extensive shear deformation. In either case, the resulting elastic anisotropy is relatively weak; but, because of the overwhelming tendency for slip to occur on basal planes, the alignment produces a much stronger anisotropy in the inelastic processes. Cole *et al.* (1996) demonstrated that the anelastic strain in field cores of aligned sea ice was in proportion to the average resolved shear stress on the basal planes. Thus a single orientation factor Ω, that converts the applied normal stress into the average basal plane shear stress, can be used to quantify the alignment effects on the dislocation-based anelasticity.

The dominant anelastic deformation mechanisms in the regime of interest (power law creep with no microcracking) are basal dislocation glide and grain boundary sliding (Cole, 1995). These mechanisms are responsible for relaxation processes observed during cyclic loading and largely govern primary creep. The dislocation-based analysis leads to the calculation of an effective mobile dislocation density, a key quantity in the model. Since the effective dislocation density is sensitive to strain and stress levels, it is a useful quantity

Table 1. Links between the physical and mechanical properties of sea ice and the associated model quantities

Physical	Mechanical	Model quantity
Brine porosity, v_b	Elastic modulus, E. Dislocation relaxation	Unrelaxed compliance, D_u. Relaxation of dislocation compliance, δD^d
Gas porosity, v_a	Elastic modulus, E	Unrelaxed compliance, D_1
Grain size, d	GB relaxation	Relaxation of GB compliance, δD^{gb}
Fabric (or half cone angle, $\angle$)	Elastic modulus, E. Dislocation relaxation	Unrelaxed compliance, D_1. Orientation factor, Ω

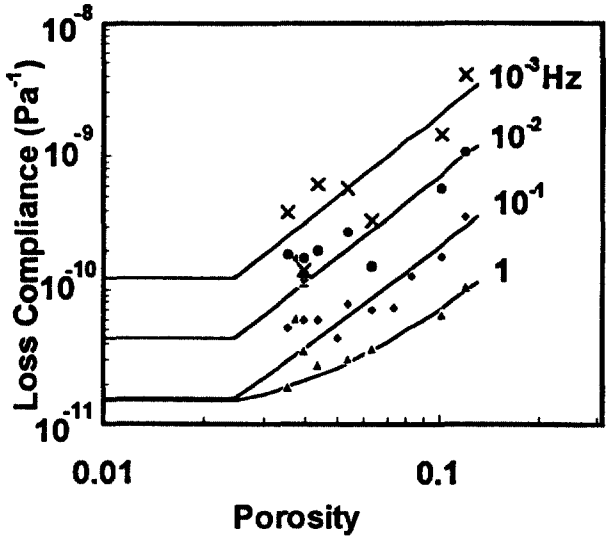

Fig. 1. Loss compliance vs. total porosity from experiments on laboratory-prepared saline ice. Cyclic loading frequencies are indicated.

for tracking the effects of previous deformation (prestrain). Experiments have shown that creep straining produces an increase in compliance (Cole, 1993) and the model ascribes this behavior to an increase in the dislocation density. This matter will be addressed in detail in a subsequent paper.

3. OVERVIEW OF THE MODEL

The anelastic straining model of Cole (1995) quantified a basal dislocation relaxation mechanism and a grain boundary sliding mechanism. The equations for the storage ($D_1(\omega)$) and loss ($D_s(\omega)$) compliancies as a function of loading frequency (ω) are:

$$
\begin{aligned}
D_1^{\mathrm{d}}(\omega) &= D_u^{\mathrm{d}} + \delta D^{\mathrm{d}}\left[1 - \frac{2}{\pi}\tan^{-1}\exp(\alpha^{\mathrm{d}} s_i^{\mathrm{d}})\right] \\
D_2^{\mathrm{d}}(\omega) &= \alpha^{\mathrm{d}}\delta D^{\mathrm{d}}\frac{1}{\exp(\alpha^{\mathrm{d}} s_i^{\mathrm{d}} + \exp(-\alpha^{\mathrm{d}} s_i^{\mathrm{d}})} \\
D_1^{\mathrm{gb}}(\omega) &= D_u^{\mathrm{gb}} + \delta D^{\mathrm{gb}}\left[1 - \frac{2}{\pi}\tan^{-1}\exp(\alpha^{\mathrm{gb}} S_i^{\mathrm{gb}})\right] \\
D_2^{\mathrm{gb}}(\omega) &= \alpha^{\mathrm{gb}}\delta D^{\mathrm{gb}}\frac{1}{\exp(\alpha^{\mathrm{gb}} s_i^{\mathrm{gb}}) + \exp(-\alpha^{\mathrm{gb}} s_i^{\mathrm{gb}})}
\end{aligned}
\tag{1}
$$

The superscripts d and gb indicate quantities pertaining to the dislocation and grain boundary relaxations, respectively: $s_i^{\mathrm{d}} = \ln(\tau^{\mathrm{d}}\omega)$ and $s_i^{\mathrm{gb}} = \ln(\tau^{\mathrm{gb}}\omega)$. The τ^i are the central relaxation times for each mechanism. Temperature enters through its effect on the relaxation times as discussed in detail in Cole (1995). The physical significance of the quantities in the model are briefly discussed in the next paragraph.

The experimental results indicated that each relaxation process can be described by a single activation energy and a distribution in relaxation times. The parameters α^{d} and α^{gb} control the width of the relaxation peaks, and thus account for the peak broadening effects of the relaxation time distribution. These values are determined from an analysis of the experimentally obtained relaxation peaks and are fixed for the ice under consideration.

Earlier findings (Cole, 1994), indicate that the grain boundary relaxation is relatively insensitive to grain size variations typically found in sea ice ($d > 3$ mm), so the grain size

Table 2. Values of model parameters

Relaxation process	Quantity	Symbol	Value
Dislocation	Relaxation of compliance (Pa^{-1})	δD^d	eqn (3)
	Peak broadening term	α^d	0.54
	Restoring stress term (Pa)	K	0.07
	Activation energy (eV)	Q^d	0.55
	Orientation factor	Ω	eqn (4)
Grain boundary	Relaxation of compliance (Pa^{-1})	δD^{gb}	4×10^{-11}
	Peak broadening term	α^{gb}	0.6
	Activation energy (eV)	Q^{gb}	1.32

dependence of that relaxation is ignored. The unrelaxed compliance (D_u^d or D_u^{gb}) is the inverse of the elastic modulus and is a function of loading direction for the case of aligned ice, fabric and the gas and brine porosities. D_u^d and D_u^{gb} are both included in the above equations for completeness. However, they each reflect the pure elastic strain and only one need be included when the effects of both relaxation mechanisms are added together. The term δD^d (the difference between the unrelaxed and relaxed compliancies) sets the magnitude of the dislocation relaxation. The following two sections are devoted to developing the dependence of δD^d and the unrelaxed compliance on the physical properties of the ice. Table 2 gives values of the model parameters. Although attention generally focuses on the dominant dislocation relaxation, the effects of the grain boundary relaxation are included in all calculations.

4. ELASTIC MODULUS CALCULATION

4.1. *Modulus of aligned ice*

The c-axes (axis of hexagonal symmetry) of individual crystals lie scattered at various angles about a common direction in aligned ice. A value of half the included scatter angle (referred to as the half cone angle for the case of three dimensions) has been used to quantify the orientation preference (Kohnen and Gow, 1979). Expressions are available for the temperature-dependent elastic constants for ice single crystals (Dantl, 1968) and for the Youngs modulus of a single crystal in an arbitrary direction of loading (Stephens, 1958). It is therefore possible to estimate the effective Youngs modulus of a polycrystal given a loading direction and the half cone angle (Sinha, 1989). The modulus thus calculated approaches the value of a polycrystal with randomly oriented grains as the half cone angle goes to 90° and approaches the appropriate single crystal value as the half cone angel goes to 0°.

The detailed fabric, ice density and ultrasonic velocity measurements conducted by Kohnen and Gow (1979) on specimens from the deep drill hole at Byrd Station, Antarctica, provide a means to verify the elastic calculations. Figure 2 shows the fabric-dependent moduli calculated from the data of Kohnen and Gow along with the model predictions. The model predictions and observed values for the horizontal orientations are in very good agreement but the observations fall below the predicted line for the vertical orientation at the lower cone angles. The difference between the theoretical and observed moduli in the vertical direction is explained by the presence of stress relief cracks that were preferentially oriented to influence the velocity measurements in the vertical direction. In general, the elastic calculations produce moduli that are in very good agreement with values obtained from ultrasonic experiments.

4.2. *Porosity effects on the modulus*

Naturally occurring ice frequently contains gas-filled voids. The effects of gas porosity on the elastic behavior of freshwater ice, and of sea ice at temperatures below the eutectic point (where no liquid brine exists), was shown in Cole (1996) to be well described for the gas porosity range of interest by $E = E(T, \angle) \times (1 - 3v_a)$. $E(T, \angle)$ is the temperature- and

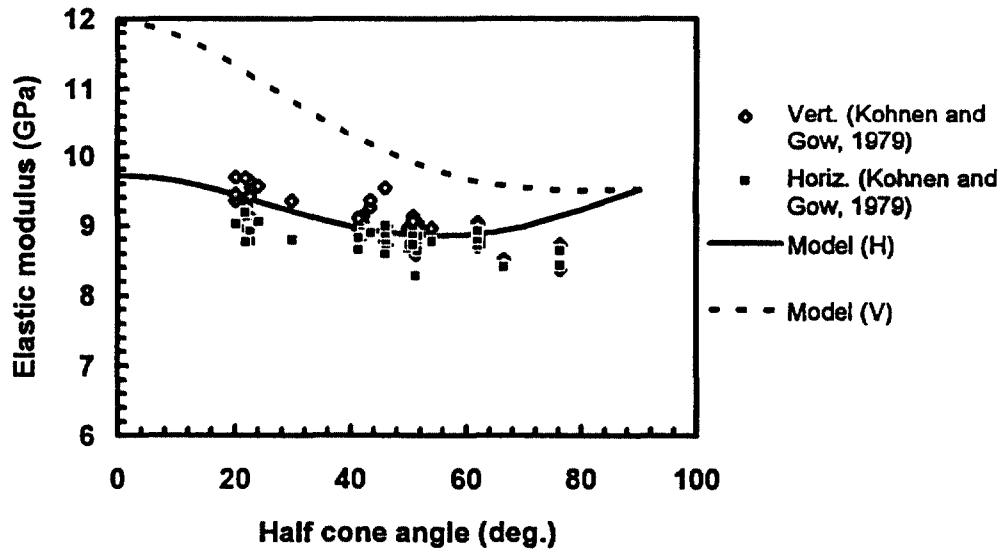

Fig. 2. Elastic modulus vs. half cone angle ($T = -10$°C). Points are calculated values using velocity and fabric from Kohnen and Gow (1979). Curves are model predictions.

fabric-dependent modulus at zero porosity and v_a is the gas porosity. The expression $(1-3v_a)$ applies to the case of noninteracting voids (Nemat-Nasser and Hori, 1993) with Poisson ratio of 1/3. It was shown by Cole (1996) to agree with available data.

The effect of brine porosity on the elastic modulus is very complex. Empirical expressions for mechanical properties ranging from tensile, compression and flexural strength to creep behavior and modulus have frequently employed a brine porosity dependence of the form $\sqrt{v_b^{-1}}$. As noted in Richter-Menge and Jones (1993) and Cole (1996), this expression accounts reasonably well for brine porosity effects over a limited range, but does not extrapolate well to higher ($v_b > 10$ ppt) or lower ($v_b < 3$ ppt) brine porosities. Although progress is being made in related areas (Shafiro and Kachanov, 1997), a detailed microstructural analysis of brine porosity effects is not yet available. As a consequence, the brine porosity effect on the elastic modulus ($f(v_b)$) is determined empirically by interpolation of the normalized relationship from Slesarenko and Frolov (1974), as shown in Fig. 3.

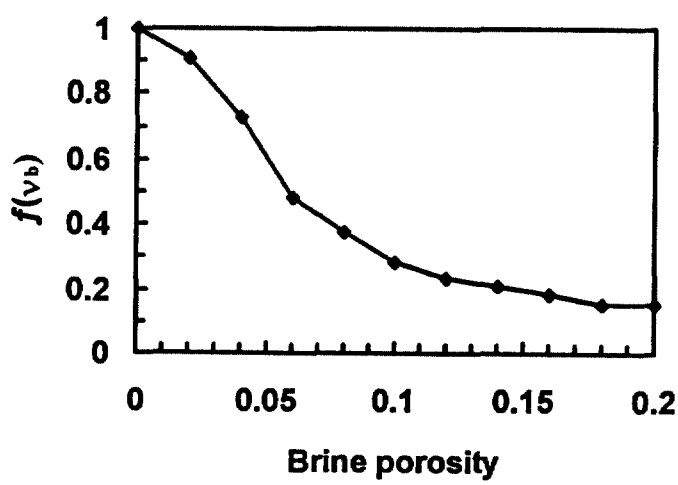

Fig. 3. Brine porosity function vs. brine porosity. Points are normalized values from the ultrasonic measurements of Slesarenko and Frolov (1974).

To summarize, the model employs the following elastic modulus calculation:

$$E = E(T, \angle) \times (1 - 3v_a) \times f(v_b) \tag{2}$$

$E(T, \angle)$ is the temperature- and fabric-dependent modulus of the inclusion-free material, $(1 - 3v_a)$ accounts for gas porosity and $f(v_b)$ accounts for brine porosity.

5. ANELASTIC STRAIN

The maximum level of anelastic straining from the dislocation mechanism is determined by δD^d, which depends linearly on the effective dislocation density ρ and the orientation factor Ω [eqn (14) in Cole, 1995]:

$$\delta D^d = \frac{\rho \Omega b^2}{K} \tag{3}$$

where the effective dislocation density ρ is now used in place of Δ in the original expression and K is the experimentally determined restoring stress constant. On the uniform stress assumption, the orientation factor Ω converts the applied normal stress to the average resolved basal plane shear stress (see Cole *et al.*, 1996). For a polycrystal of n grains, each with area A_i, with the direction of applied stress making an angle φ_i with the basal plane normal and an angle λ_i with the slip direction, the orientation factor is determined by:

$$\Omega = \sum_{i=1}^{n} \frac{A_i}{A} \cos(\lambda_i) \cos(\varphi_i) \tag{4}$$

where $A = \Sigma_{i=1}^{n} A_i$. The orientation factor can thus be calculated directly from microstructural information.

Since Ω can be calculated, K is determined experimentally, and b is known, eqn (3) provides a relationship between δD^d and the mobile dislocation density ρ. Since experimental observations have provided a relationship between δD^d and specimen porosity v, an important link between the physical and mechanical properties can be established by empirically relating the initial mobile dislocation density and v:

$$\text{For } v > 0.024, \rho_0(v) = 5 \times 10^{11} v^2 \text{ m}^{-2}$$

$$\text{For } v \leqslant 0.024, \rho_0(v) = 3 \times 10^8 \text{ m}^{-2} \tag{5}$$

In eqn (5), $\rho_0(v)$ is the initial or grown-in dislocation density. The threshold value of $\rho_0(v)$ has been revised downward slightly from 4×10^8 m^{-2} reported in Cole (1996). The subscript is employed to distinguish the initial value from the prevailing value during straining, which can increase above ρ_0 depending on strain and stress level. The model employs a threshold strength of the dislocation relaxation since δD^d for saline ice is not expected to drop below the freshwater ice value as $v \to 0$. In eqn (5), the value of $v = 0.024$ corresponds to this threshold, and $\rho_0(v) = 3 \times 10^8$ m^{-2} is an average value calculated from the experimentally observed compliance of five columnar-grained freshwater ice specimens. The relationships in eqns (3) and (5) provide the sought-after link between anelastic strain and a fundamental physical property.

The curves in Fig. 1 result from employing eqn (5) in the model predictions. The lower-frequency ($\leqslant 10^{-1}$ Hz) curves are dominated by the dislocation relaxation mechanism and clearly show the power law dependence [eqn (5)] above the porosity threshold ($v = 0.024$). The influence of that mechanism weakens at higher frequencies, and the grain boundary relaxation mechanism becomes relatively more important. This causes the increasing branch of the 1 Hz curve in Fig. 1 to deviate from the power law behavior indicated in eqn (5).

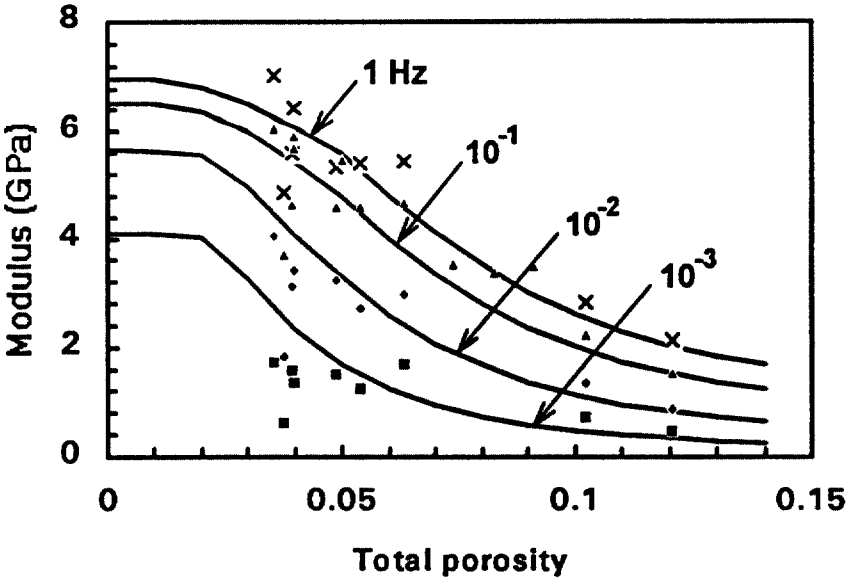

Fig. 4. Modulus vs. total porosity. Points are from experiments on laboratory-prepared saline ice and curves are model predictions. Cyclic loading frequencies are indicated.

Figure 4 compares the porosity dependence of the model predictions for the steady-state modulus with experimental observations. The curves in Fig. 4 were calculated from $(\partial\sigma/\partial\varepsilon)_{\sigma=0}$ from the stress/strain relationships predicted by the model, excluding initial transient effects. The points were determined from the experimentally obtained stress/strain data. They are average values for the second and higher loading cycles and thus do not include the transient effects evident in the first loading cycle. Figure 5 shows a comparison for the alignment effects observed on field cores of aligned first-year sea ice. The moduli for a half cone angle of 10° in Fig. 5 were included to demonstrate the validity of the predictions for ice having a very low resolved basal plane shear stress. The points are from

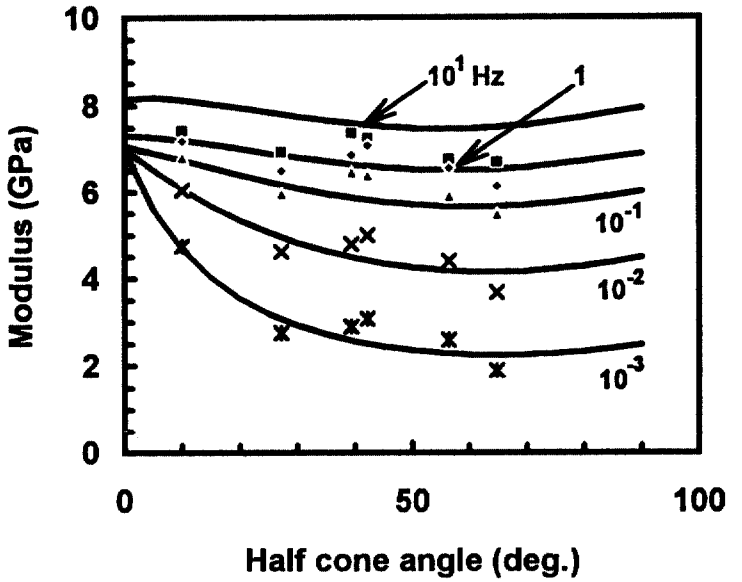

Fig. 5. Modulus vs. half cone angle. With the exception of the moduli at a half-cone angle of 10°, data points are from laboratory experiments on horizontal field cores of aligned first-year ice. The moduli for a half cone angle of 10° are from a vertical specimen of laboratory-prepared ice shown to illustrate extreme alignment effects.

a vertically oriented specimen of laboratory-prepared saline ice. In both Figures, the model predicts the appropriate magnitude and trends evident in the experimental data reasonably well.

6. DISCUSSION

Calculation of fabric and gas porosity effects on the elastic modulus is relatively straightforward and produces moduli that are in good agreement with observations in the literature. Although it would be preferable to use such a deterministic approach in the assessment of the brine porosity effects on the elastic modulus, such a calculation has apparently not yet been made for sea ice. The empirical $f(v_b)$, however, adequately describes the brine porosity effects on the elastic modulus, has a sound experimental basis and brings the model predictions well in line with the cyclic loading observations. Additionally, this approach provides a valid prediction of the modulus over a very wide range in brine porosity.

Even in unstrained ice with low salinity (1–2 ppt), the grown-in dislocation density is so high that individual dislocations cannot be resolved by means of synchrotron X-ray topography (Baker, 1995). It has therefore proved difficult to establish the physical link between brine porosity and the initial dislocation density of the material [eqn (5)] by direct observation. Future efforts will focus on establishing when (during or subsequent to ice growth) the dislocations are introduced into the ice lattice, with the intention of isolating the process responsible for generating them.

With regard to the threshold dislocation density employed in eqn (5), this value ($\rho_0(v) = 3 \times 10^8\,\mathrm{m}^{-2}$) may be subject to revision as the freshwater ice data base used in its calculation expands. However, small variations in the threshold value will not affect the model predictions at the higher porosities normally encountered.

Although not emphasized here, the time/temperature history of the ice has a strong influence over the physical and therefore mechanical properties of sea ice. As a consequence of brine drainage, sea ice that has survived at least one melt season (multi-year ice) typically has a lower salinity than first-year ice. It remains to be seen whether such ice will exhibit the same brine porosity-compliance relationship found for laboratory-prepared ice that was initially grown with a low salinity.

With the exception of $f(v_b)$, the model is based on experimental results for laboratory-prepared saline ice. Other than the experimental conditions and fabric data, the model requires only the salinity and density of the ice. It is therefore encouraging to note the good agreement between the model predictions and the experimental data from the field cores of aligned first-year sea ice (Fig. 5). Efforts are continuing to further verify the model on the basis of experiments on field cores. It is noted in passing that preliminary work comparing the internal friction (ratio of the dissipated strain energy during a cycle of loading to the maximum stored strain energy) predicted by the model with results from the large-scale in-situ experiments mentioned above has produced very good agreement as well.

7. CONCLUSIONS

Based on the foregoing analysis and the supporting laboratory experimental work, it may be concluded that it is possible to separate and quantify the effects of brine and gas porosity on the elastic and anelastic straining of sea ice. Gas porosity effects on the elastic modulus are adequately modeled by applying a factor of $(1 - 3v_a)$ to the pore-free modulus. For the case of aligned polycrystalline ice, estimations of the effective elastic properties based on the temperature-sensitive single crystal moduli proved to be in good agreement with values obtained from ultrasonic experiments in the literature.

Brine porosity effects on the elastic modulus are complex and it is currently necessary to employ an empirical factor based on experimental results in the literature. There is a strong correlation between brine porosity and basal plane compliance in laboratory-prepared saline ice, although the underlying physical mechanism for this correlation is unclear. A dislocation-based analysis of the anelastic relaxation leads to a calculated basal plane

dislocation density that increases with the square of the brine porosity. This relationship provides an important link between the physical properties of sea ice and the anelastic relaxation process.

Acknowledgements—This work was conducted under the Office of Naval Research, Sea Ice Mechanics Initiative, Grant nos N0001495MP30001 and N0001496MP30021. The author expresses his appreciation to Drs Thomas Swean, Thomas Curtin and Yapa Rajapakse of ONR for their support. He also gratefully acknowledges helpful discussions with Prof. Richard Schaperty (U.T.—Austin), Dr A. J. Gow (U.S.A.—CRREL), Profs. W. Weeks and L. Shapiro (U.A.—Fairbanks) during the course of this work.

REFERENCES

Adamson, R. M. and Dempsey, J. P. (1996) Large-scale in-situ Arctic cyclic, creep recovery and fracture experiments. *Proceedings of the IAHR 13th International Symposium on Ice*, Vol. I. pp. 102–109. Beijing.

Baker, I. (1995) Personal communication.

Cole, D. M. (1993) The effect of creep on the constitutive behavior of saline ice at low strains. In *Ice Mechanics 1993, Proceedings 1st Joint Mechanics Meeting of ASME, ASCE and SES*, June 6–9, AMD-vol. 163, pp. 261–272. Charlottesville, VA.

Cole, D. M. (1994) The effect of temperature and microstructure on the constitutive behavior of ice at low strains. *Proceedings of the IAHR 12th International Ice Symposium*, Vol. 3, pp. 1051–1058. Trondheim, Norway.

Cole, D. M. (1995) A model for the cyclic loading of saline ice subjected to cyclic loading. *Phil. Mag. A* **72**(1), 231–248.

Cole, D. M. (1996) On the relationship between the physical and mechanical properties of sea ice. *Proceedings of the 13th International Symposium on Ice*, Vol. III. Beijing, in press.

Cole, D. M. and Durell, G. D. (1995) The cyclic loading of saline ice. *Phil. Mag. A* **72**(1), 209–230.

Cole, D. M., Johnson, R. A. and Durell, G. D. (1996) The cyclic loading response of aligned first-year sea ice. *Proceedings of the 13th International Symposium on Ice*, Vol. I, pp. 1–7. Beijing.

Cole, D. M., Shapiro, L. H., Weeks, W. F., Dempsey, J. P., Adamson, R. M., Petrenko, V. F. and Gluschenkov, O. V. (1995) Overview of a recent program on the mechanical properties of sea ice. *J. Cold Regions Eng.* **9**(4), 291–234.

Cox, G. F. N. and Weeks, W. F. (1983) Equations for determining the gas and brine volumes in sea-ice samples. *J. Glaciol.* **29**(102), 306–316.

Dantl, G. (1968) Elastic moduli of ice. In *Physics of Ice, Proceedings of the International Symposium on Physics of Ice*, Ed. N. Riehl, B. Bullemer and H. Engelhardt, pp. 223–230.

Dempsey, J. P (1996) Scale effects on the fracture of ice. In *The Johannes Weertman Symposium*, Ed. R. J. Arensault, D. Cole, T. Gross, G. Kostorz, P. Liaw, S. Parameseran and H. Sizek, pp. 351–361. The Minerals, Metals and Materials Society.

Kohnen, H. and Gow, A. J. (1979) Ultrasonic velocity investigations of crystal anisotropy in deep ice cores from Antarctic. CRREL Report 79–10, 16 p.

Nemat-Nasser, S. and Hori, M. (1993) *Micromechanics: Overall Properties of Heterogeneous Materials*. North-Holland, New York, 687 p.

Peyton, H. R. (1966) Sea ice strength. Geophysical Institute, University of Alaska, Report UAG-182, 187 p.

Picu, R. C., Gupta, V. and Frost, H. J. (1994) Crack nucleation mechanisms in saline ice. *J. Geophys. Res.* **99**(B6), 11,775–11,786.

Richter-Menge, J. A. and Jones, K. F. (1993) The tensile strength of first-year sea ice. *J. Glaciol.* **39**(133), 609–618.

Shafiro, B. and Kachanov, M. (1997) Materials with fluid-filled pores of various shapes: effective elastic properties and fluid pressure polarization. *International Journal of Solids and Structures* **34**(27), 3517–3540.

Sinha, N. K. (1989) Elasticity of natural types of polycrystalline ice. *Cold Regions Sci. Technol.* **17**, 127–135.

Slesarenko, Yu, E. and Frolov, A. D. (1974) Comparison of elasticity and strength characteristics of salt-water ice. *IAHR Symposium on Ice and its Action on Hydraulic Structures* **2**, 85–86, Leningrad.

Stephens, R. W. B. (1958) The mechanical properties of ice. II. The elastic constants and mechanical relaxation of single crystal ice. *Advances in Physics* **7**, 266–275.

Weeks, W. F. and Gow, A. J. (1979) Crystal alignments in the fast ice of arctic Alaska. CRREL Report 79–22, 21 p.